HHS Public Access

Author manuscript

SLAS Technol. Author manuscript; available in PMC 2020 May 14.

Published in final edited form as:

SLAS Technol. 2017 December ; 22(6): 646–661. doi:10.1177/2472630317726050.

Adaptation of a simple microfluidic platform for high-dimensional quantitative morphological analysis of human mesenchymal stromal cells on polystyrene-based substrates

Johnny Lam[1], **Ross A. Marklein**[1], **Jose A. Jimenez-Torres**[2], **David J. Beebe**[2], **Steven R. Bauer**[1], **Kyung E. Sung**[1,*]

[1]Division of Cell and Gene Therapies, Center for Biologics Evaluation and Research, Food and Drug Administration, Silver Spring, MD, USA

[2]Department of Biomedical Engineering, University of Wisconsin-Madison, Madison, WI, USA

Abstract

Multipotent Stromal Cells (MSCs, often called mesenchymal stem cells) have garnered significant attention within the field of regenerative medicine due to their purported ability to differentiate down musculoskeletal lineages. Given the inherent heterogeneity of MSC populations, recent studies have suggested that cell morphology may be indicative of MSC differentiation potential. Toward improving current methods and developing simple yet effective approaches for the morphological evaluation of MSCs, we combined passive pumping microfluidic technology with high dimensional morphological characterization to produce robust tools for standardized high throughput analysis. Using ultraviolet (UV) light as a modality for reproducible polystyrene (PS) substrate modification, we show that MSCs seeded on microfluidic straight channel devices incorporating UV exposed substrates exhibited morphological changes that responded accordingly to the degree of substrate modification. Substrate modification also effected greater morphological changes in MSCs seeded at a lower rather than higher density within microfluidic channels. Despite largely comparable trends in morphology, MSCs seeded in microscale as opposed to traditional macroscale platforms displayed much higher sensitivity to changes in substrate properties. In summary, we adapted and qualified microfluidic cell culture platforms comprising simple straight channel arrays as a viable and robust tool for high-throughput quantitative morphological analysis to study cell-material interactions.

Keywords

microfluidics; MSC; mesenchymal stromal cells; high dimensional morphological analysis; substrate modification

*Corresponding Author, kyung.sung@fda.hhs.gov.

Disclosure of Potential Conflicts of Interest

Dr. David J. Beebe holds equity in Bellbrook Labs LLC, Tasso Inc., Stacks to the Future LLC, Lynx Biosciences LLC, Onexion Biosystems LLC, and Salus Discovery LLC.

Supplemental material link https://journals.sagepub.com/doi/suppl/10.1177/2472630317726050

Figures and tables https://journals.sagepub.com/doi/figure/10.1177/2472630317726050?

Introduction

Since their discovery [1], bone-marrow derived mesenchymal stromal cells (MSCs), otherwise referred to as mesenchymal stem cells, have gained significant attention as a potential cell source for clinical applications in regenerative medicine for their apparent ability to differentiate into cells of osteogenic, chondrogenic and adipogenic lineages. Despite this, recent studies have shown that MSC subpopulations, as well as MSCs derived from different donors, display different capacities for proliferation and differentiation [4]. Due to this well-documented functional heterogeneity, efforts have emerged to characterize MSCs at a higher single-cell resolution in order to gain a better understanding of the heterogeneity inherent to different cell subpopulations and MSCs derived from different donors and manufacturing conditions. Of note, some promising results suggest that individual cellular characteristics such as morphological profiles may be reflective of MSC osteogenic differentiation potential [5].

Since both cell and nuclear morphology can be indicative of MSC differentiation potential, recent attempts at developing simple yet effective approaches have involved the high throughput characterization of morphological differences between MSC subpopulations as a means of predicting MSC potency [5]. However, such methods often utilize standard cell culture open-well formats that fail to model physiologically relevant microenvironmental conditions. Indeed, cells and their internal structures operate within milieus that have physical dimensions at the microscale, which can be simulated using microfluidic technologies [7]. The growing adaptation of miniaturized tools for biological inquiry via microfluidic technology provides the ability to address such shortcomings [8]. In adapting microfluidics for cell culture, it becomes important to consider how physical differences in culture platforms as well as the translation of cell culture practices will affect cell behavior [9]. A thorough understanding of how cells morphologically interact with their substrates as influenced by the physical scale of the culture environment (micro- versus macroscale) will elucidate intricacies that may enable the creation of a robust method for predicting the behavior of MSCs based on their morphology.

In the present study, we cultured MSCs in established microfluidic straight channel devices compatible with high-throughput assays [10] as a simple method for characterizing cell morphological response to changes in substrate properties. Here, we used ultraviolet (UV) exposure, which is commonly employed as a practical method for microfluidic device sterilization, as a modality for reproducible substrate modification. We found that exposure to a constant UV source increases the hydrophilicity of polystyrene (PS) substrates in an exposure time-dependent fashion, which subsequently effects changes in the morphology of MSCs cultured on these substrates. We further demonstrated that UV exposure effected changes in MSC morphological parameters to a greater extent when the MSCs were seeded at a lower seeding density in microfluidic straight channels versus traditional well plates. We showed that despite similar trends in morphological response on identically treated PS substrates, MSCs cultured in a microfluidic setting consistently exhibited higher sensitivity to substrate properties. This suggests that PS substrate surface modification by UV exposure may impart nuanced effects on MSC behavior depending on the physical scale of the culture environment. As a result, we qualified microfluidic straight channels as a simple and viable

platform with high adaptability for high-throughput cell morphological assays. Together, these results have important corollaries for the manufacturing processes and single-cell testing of MSCs for cell-based therapies.

Materials and Methods

Microfluidic Device Fabrication

The microfluidic devices used in this study were fabricated using soft lithography and rapid prototyping. Briefly, SU-8 100 negative photoresist was spun to generate a 250 micron thick layer on a 6-in silicon wafer and cured with UV light to form the layer for the channels. A second 250 micron thick layer of SU-8 for the ports was then spun and cured to form the master replica mold. Elastomeric polydimethylsiloxane (PDMS, Sylgard 184 Silicon Elastomer Kit, Dow Corning) was cast over the SU-8 master and cured under compression. PDMS microchannels were first fabricated as arrays comprising 192 identical straight microchannels following established procedures [10a, 11], where individual channels were 5.75 L x 0.75 W x 0.25 H (mm) in dimension. These microfluidic straight channel arrays take advantage of passive pumping for media exchange [12]. Smaller arrays of identical microchannels were cut out from the larger array as needed, sterilized with 70% ethanol, and then reversibly bonded to non-treated bacteriological grade PS substrates (bgPS; Nunc) or tissue culture-treated PS substrates (tctPS; BD Falcon). Bonded devices were air-dried prior to cell-seeding.

MSC Expansion

Human bone marrow-derived MSCs, were purchased from RoosterBio Inc. (Frederick, MD, www.roosterbio.com) at passage 1. MSCs were culture expanded at an initial plating density of 8.33×10^5 cells/T225 flask (~3,700 cells/cm^2) following the protocol and using the growth media as provided by the manufacturer (hMSC High Performance Media Kit, RoosterBio Inc.). Upon reaching approximately 80% confluence, cells were then trypsinized and re-plated at the same initial plating density of 8.33×10^5 cells/T225 flask, which is regarded as one “passage.” MSCs were continuously expanded for multiple passages, with a small portion of cells being cryopreserved in freezing medium (30% fetal bovine serum (FBS, JM Bioscience, San Diego, CA, www.jmbioscience.com), 5% dimethyl sulfoxide (DMSO, Sigma, St. Louis, MO, www.sigmaaldrich.com), 1% l-glutamine, 1% penicillin-streptomycin in alpha minimum essential media (alpha-MEM, Life Technologies) at each passage throughout the expansion process. MSCs from passage 2 were used for the studies described herein.

UV Irradiation/Sterilization of Polystyrene Substrates

For this study, PDMS microchannels were sterilized by soaking in 70% ethanol followed by washing with sterile phosphate buffered saline (PBS). The PS substrates were sterilized separately by exposure at a uniform distance from the UV light (75 W, 254 nm) within a standard laminar flow biosafety cabinet (SterilGARD e^3 SG603A-HE, The Baker Company, Sanford, ME) for the times indicated in the experimental design. The irradiance of the UV light source from the biosafety cabinet at the location of substrate treatment was measured to be 392.9 μW/cm^2, which meets the minimum acceptable irradiance of 40 μW/cm^2 [15].

Sterilized components were then assembled in the sterile laminar flow hood and left to air-dry prior to cell seeding.

Measuring Contact Angles

The contact angles of water droplets on various PS substrates as effected by prior UV exposure were measured using a goniometer (Standar goniometer, ramé-hart Inc, Mountain Lakes, NJ) following standard methods [13]. Briefly, the static contact angles from both sides as well as the height of distilled water drops were measured for each sample at 5 different locations and averaged. Corresponding contact angles from bgPS substrates were also obtained as a comparison. Contact angle measurements were used as indicators of surface hydrophilicity.

Cell Culture and Seeding

Prior to cell seeding, passage 2 MSCs were first thawed and cultured in growth media (alpha-MEM, 16% FBS, 1% l-glutamine, and 1% penicillin-streptomycin) until approximately 80% confluency. MSCs were then trypsinized and used to prepare single cell suspensions of the appropriate concentrations in order to achieve the desired microchannel surface densities as outlined in the Experimental Design section.

To seed cells into microchannels, the appropriate media was first added to the microchannels (~6 μL), which were then put into the incubator while cells were prepared. Once the cell suspensions were prepared at the desired concentrations, 2.5 μL of the cell suspension was then added to the microchannels via passive pumping. For the macroscale cultures, cells were seeded into wells of a 12-well plate at concentrations necessary to achieve corresponding cell surface densities between the two culture platforms. It should be noted that while the corresponding wells and microchannels share similar surface densities, volume densities are much higher for the microscale cultures [14]. Seeded microchannels and well plates were then placed in a humidified incubator at 5% CO_2 and 37° C. 24h after seeding into their respective culture platforms, cells were fixed and stained for analysis.

Experimental Design

To confirm the effects of UV exposure on the wettability of various PS substrates, bgPS and tctPS substrates were exposed to UV light from the biosafety cabinet for 0, 2, 4, and 16h as described and then the contact angles were measured. A subset of UV treatment durations (0, 4, and 16h) was then selected (Table 1a) in order to evaluate how substrate UV exposure affects the morphology of subsequently seeded MSCs. The first experiment investigated MSC morphological changes on bgPS surfaces in a microscale environment, where it is hypothesized that short durations (up to 2h) of UV irradiation will actually enhance cell spreading on bgPS. Specifically, MSCs were loaded at two different seeding densities (10000 or 50000 cells/cm^2) into microfluidic channels incorporating bgPS substrates (bgPS microchannels) that have been exposed to UV for 0, 2, 4, or 16h. Serum-free media was used to remove any potential confounding effects on cell adhesion from the adsorption of exogenously delivered proteins.

A full factorial design (Table 1b) was then utilized to investigate the main and combined effects of UV surface treatment (0, 4, 16h), growth media composition (SF, 2% FBS, 16% FBS), and cell seeding density (5000 or 10000 cells/cm^2) on the morphology of the MSCs cultured in microfluidic channels comprising tctPS substrates. For tctPS microchannels, the range of cell densities was reduced from 10000–50000 to 5000–10000 cells/cm^2 in order to avoid overconfluence and to enable morphological analysis of MSCs at single-cell resolution. To compare differences in cell-substrate interactions between macroscale and microscale environments, a subset of the groups outlined in Table 1b were additionally run in parallel in standard 12-well cell culture plates (Table 1c).

Fixation, Staining, and Image Acquisition

Cells seeded within microchannels and on well plates were fixed and stained following established protocols provided by the manufacturer. Briefly, cells were first washed with PBS, fixed with 4% paraformaldehyde (in PBS) for 20 min at room temperature, washed again with PBS, and then permeabilized with 1X BD Perm/Wash buffer (BD Biosciences, San Jose, CA, www.bdbiosciences.com) for 5 min at room temperature. After permeabilization, cells were stained for actin (1:40 dilution, AlexaFluor 488 Phalloidin, green, Invitrogen by Life Technologies, Saint Aubin, France) and nuclei (1:500 dilution, 4’,6-diamidino-2-phenylindole (DAPI), blue, Thermo Fisher Scientific) for 20 min at room temperature. Cells were then washed with PBS and imaged. Images for qualitative assessment were obtained using an EVOS AMG microscope (EVOS Advanced Microscope Group). Whole microchannel images (4 individual microchannels per group) for quantitative morphological analysis were acquired using an inverted Nikon Ti-S microscope with automated stage (Prior Scientific, Rockland, MA, www.prior.com) and filters (Chroma Technology, Bellows Falls, VT, www.chroma.com) and stitched using the provided software (NIS, Nikon). Images of cells seeded on well plates (four wells per group; 25 random points per well) were also imaged using the Nikon Ti-S microscope. A brief schematic of the methodology is shown in Figure 1. A LIVE/DEAD staining kit (Invitrogen) was also utilized to qualitatively assess the viability of MSCs seeded onto UV-exposed PS substrates within microchannels (Supplemental Figure 1).

Quantitative Morphological Analysis

For each experimental group, each straight microchannel (8 individual microchannels per group for bgPS microchannels and 4 individual microchannels per group for tctPS microchannels) representing an independent biological replicate was imaged using automated microscopy and the individual images were then stitched to provide a single image of the entire microchannel (excluding the inlet and outlet ports), which was then used for morphological analysis. Images of cells seeded on conventional well plates (four wells per group; 25 random points per well) were obtained and assessed without stitching. Following previously established procedures [5a], automated quantification of several key cellular shape features was performed using the open source image analysis software CellProfiler [16] to provide a high-dimensional morphological characterization of each cell. To first compare basic trends in cell morphology, we quantitatively analyzed the shape area, eccentricity, form factor, and the solidity of individual cells from the images collected for each group. The cellular area (the number of pixels in the identified shape) and eccentricity

(the degree of elongation of the identified shape) provide for an assessment of the degree of cell spreading, whereas the form factor (or circularity, calculated as 4*pi*area/perimeter^2, which equals 1 for a perfectly circular object) and solidity (proportion of pixels in the convex hull that are also in the identified shape) allow for an understanding of morphological irregularities. In order to thoroughly compare differences in MSC morphological responses on microscale and macroscale culture platforms, the aforementioned shape features were aggregated with 10 additional shape features (listed and defined in Supplemental Table 1) using principal component analysis (PCA). PCA permits the reduction of high-dimensional multivariate data into a smaller number of artificial principal components, which represent uncorrelated linear combinations of optimally-weighted observed variables that capture maximal variance in the original dataset [5]. From the analyses, only the first two principal components were selected as they accounted for at least 70% of the cumulative explained variance in their respective datasets. The CellProfiler algorithm (pipeline) used to analyze morphology can be viewed in Supplemental Table 2.

Statistical Analysis

Given the large amount of samples as well as the presence of extreme values for each group, the morphological characteristics for each experimental group were determined by evaluating only the range of samples that fall within the 1st and 3rd quartile values based on the cell spreading area feature of whole datasets derived from each individual image set of each group. The area was used (instead of the other aforementioned shape features) as this feature consistently allowed for the identification of small debris and background from imaged cells. Table 1 provides the total n number of cells analyzed for each UV treatment group for each study. A mixed model was utilized to account for the individual-level observation of cells as well as the group-level effects of the independent microchannels/wells from which the cells are derived [17]. Statistically significant differences in morphological characteristics between groups were analyzed using the statistical software JMP12 (SAS Cary, NC, www.jmp.com). The main effects and interaction analysis of the full factorial studies were also performed using JMP12, where the raw statistical results of the effects tests from the analysis are presented in Supplemental Table 3–5. To further assess high dimensional morphological dataset including all 14 shape parameters, PCA was also performed using JMP12 to uncover any distinct overall differences that correlate with UV surface treatments, cell media composition, and/or cell seeding densities. All data were analyzed using ANOVA followed by Tukey's post-hoc test, where a confidence interval of 95% was used and differences were considered significant when $p<0.05$.

Results and Discussion

Wettability of unexposed and UV-exposed PS substrates

A comparison of the 'water in air' contact angle, which is used as an indicator of hydrophilicity, between tctPS and bgPS surfaces showed that bgPS consistently maintained both greater contact angles as well as droplet heights (i.e., less hydrophilic) at all tested durations of UV exposure (0, 2, 4, and 16h). For the bgPS substrates, both the water contact angle and the droplet height continued to decrease with increasing durations of UV exposure, indicating a gradual increase in hydrophilicity. Specifically, the contact angle of

unexposed bgPS controls (0h) decreased from 80.84º±2.02 to 77.65º±2.45 at 2h of exposure, to 73.23º±1.14 at 4h of exposure, and finally to 57.28º±2.88 following 16h of UV exposure. The water droplet height followed a similar trend as it gradually decreased from 1.83 mm ±0.05 on unexposed bgPS surfaces to 1.41 mm±0.06 after 16h of UV exposure. This can be observed in Table 2.

Unlike bgPS substrates, tctPS substrates are usually plasma treated in order to overcome the inherent hydrophobicity of unmodified PS that resists cell attachment [18]. As expected, control tctPS substrates displayed lower contact angles when compared to their bgPS counterparts (Figure 2). However, the water contact angles and droplet heights of tctPS surfaces did not further decrease following 2h of UV exposure. This could be potentially due to the saturation of the tctPS surface with oxygen species caused by a combination of both prior plasma treatment and subsequent UV irradiation. Previous studies characterizing the chemical composition of PS substrates using X-ray photoelectron spectroscopy have reported that the carbon-to-oxygen species ratio (C:O) (oxygen containing species include C-O-C, COH, C=O, and COO- groups) of tctPS surfaces typically range anywhere between 82:18 to 85:15, whereas the C:O ratio of bgPS surfaces range between 94:6 to 97:3 [19]. For comparative measures, it was also demonstrated that the treatment of pure electrospun PS scaffolds with argon plasma altered the C:O ratio from essentially all carbon species to roughly 80:20 C:O [19]. As an increase in the number of oxygen containing species translates to an increase in surface charge and hydrophilicity, the decreasing water contact angles observed for bgPS substrates in the present study may be due to the formation of such oxygen species (between air and PS) caused by increasing UV exposure durations.

Given the prevalence of PS as a substrate for cell culture [20], the effects of various manufacturing processes on PS properties have been extensively studied. Despite the favorable material and optical properties which make PS suitable for numerous biological applications, the polymer itself is highly susceptible to photodegradation. When exposed to UV light in the presence of air, PS undergoes photooxidative changes that yield free radicals capable of reacting with other reactive species (from the air or degrading PS). The generation of various aromatic compounds and other PS derivatives [21] is evidenced by changes in spectral properties via the formation of new optical centers [22] as well as gradual embrittlement of the material. Because the photodegradation of PS will certainly alter its material properties, it is important to consider the effects of changes in substrate properties on the behavior of seeded MSCs since UV light (installed in virtually all laminar flow biosafety cabinets) still remains the leading method of sterilization for tools used for cell culture [23] . Even though ultraviolet (UV) irradiation can be used, exposure of assembled PDMS/PS microfluidic devices to UV light may not be the most effective means of sterilization as PDMS is not transparent to UV light [24]. This becomes especially important for microscale platforms incorporating PS substrates, where cells can respond differently to experimental stimuli just given the physical scale difference (keeping all other conditions the same) when compared to macroscale environments [8a, 9a, 9c, 25].

We therefore performed the following factorial experiments aimed to understand how UV irradiation (and the duration of UV irradiation) effects changes in MSC morphology based on the type of PS substrate, the cell seeding density, as well as the cell culture media

composition used. We hypothesize that UV irradiation will increase the hydrophilicity of the PS substrates, which will influence changes in cell morphology of subsequently seeded MSCs within microchannels but not necessarily to the same extent in macroscale culture platforms due to volume density differences in culture environment. Although the following experiments utilized UV irradiation as a simple modality for substrate modification, the analytical methods and platform presented can be easily applied to interrogate cell morphological response to various other forms of modified substrates.

Evaluation of cell morphological features of MSCs in microfluidic channels incorporating unexposed and UV-exposed bgPS substrates

The first set of experiments evaluated both the effects of substrate UV exposure and the initial cell seeding density on the morphology of MSCs seeded in bgPS microchannels. Generally, MSCs seeded in bgPS microchannels at both low and high cell densities exhibited cell morphological features that were dependent on the substrate UV exposure duration. From the quantitative analysis, the cell spreading area of seeded MSCs decreased with increasing durations of substrate UV exposure (Figure 3A). Despite this, MSCs seeded in 16h UV bgPS microchannels were less elongated in shape (decreased eccentricity) and possessed more regular boundaries (increased solidity, less filopodial extensions) when compared to all other bgPS groups (Figure 3B and 3D). MSCs seeded on 2h UV bgPS surfaces were less circular (decreased form factor) when compared to those on 16h UV bgPS substrates (Figure 3C). A formal main effects analysis (Supplemental Table 3) further revealed several interactions between the factors of substrate UV exposure duration and initial cell seeding density on all of the quantified morphological features (Supplemental Figure 2). Notably, MSCs seeded at a lower density in 2h UV bgPS microchannels exhibited larger spreading areas when compared to those from the non-irradiated controls; this effect was absent for MSCs seeded at a higher initial density. These cross effects demonstrate that within microscale environments, cells seeded at lower densities are more sensitive to substrate modifications, whereas the response of cells seeded at higher densities is likely more dominated by paracrine effects due to increased cell proximity. While these data demonstrate that UV exposure of bgPS prior to cell seeding reduces the degree of cell spreading in general, short durations of substrate UV exposure may actually enhance some attributes of cell morphology (i.e. increased spreading area) on bgPS (non-tct) surfaces. The morphology of MSCs from the various bgPS groups is shown in Figure 4.

From the PCA of the bgPS morphological dataset, a plot comparing the principal component 1 (PC1) and PC2 scores, which captured 42.2% and 34.7% of the total variance, respectively, revealed notable insights into the MSC morphological response to changes in substrate properties as influenced by the initial cell seeding density. Specifically, MSCs seeded at a lower density (10000 cells/cm^2) on bgPS substrates that were exposed to short durations of UV (up to 2h) were morphologically different when compared to MSCs seeded onto 16h UV bgPS substrates (Figure 3E). Two morphologically distinct MSC subpopulations can be discerned from the PC scores plot for the intermediate 4h UV bgPS group; one subpopulation shares similar morphology to the 0h and 2h UV bgPS groups while the other subpopulation possesses overall morphology similar to the 16h UV bgPS group. These morphological trends, however, were absent for MSCs seeded within bgPS

microchannels at the higher initial density of 50000 cells/cm^2 (Figure 3F). This could be possibly explained by the increased paracrine effects of MSCs at higher seeding densities, resulting in a greater adsorption of secreted proteins that overcame variations in cell-substrate interactions. Taken together, these data substantiate the presence of multiple MSC subpopulations that display unique morphological characteristics in response to changes in substrate properties.

Given that the morphology of MSCs can be indicative of their differentiation potential [5], the ability to discern MSC subpopulations with unique morphological signatures would be important to the success of a predictive assay. As each principal component can be described as a linear composite of optimally-weighted variables, the coefficients representing the contribution of each parameter for principal components capturing the highest variance may be utilized to select for morphological parameters that are most dominant in separating out cell subpopulations. In addition to characterizing MSC heterogeneity, these data also demonstrate the potential to apply simple microscale platforms combined with high-dimensional morphological analyses in order to refine conditions in the manufacturing of cells to identify and enrich for morphologically distinct cell subpopulations. Indeed, this platform may be adapted in future work to assess whether MSCs isolated from other donors and tissue sources have similar morphological responses to other forms of substrate modifications.

Evaluation of cell morphological features of MSCs in microfluidic channels incorporating unexposed and UV-exposed tctPS substrates

Unlike bgPS, commercial tctPS substrates for cell culture are typically pre-treated with either gas-plasma under vacuum or corona discharge in order to render the surface hydrophilic (primarily via the generation of carboxyl groups) for increased cell adhesion [26] and then sterilized with gamma irradiation by the manufacturer. However, a rapidly growing number of bioengineering applications involves the use of custom cell culture devices incorporating tctPS substrates that require additional sterilization (either with UV or ethylene oxide gas) prior to use. The effectiveness of various sterilization modalities used to additionally decontaminate engineered devices intended for cell culture may often prove inadequate and may even influence experimental outcomes [27]. Although UV was simply used as a method for substrate modification for our studies, this becomes an important consideration especially since UV light, while seemingly innocuous, may actually influence cell behavior in nuanced ways that could have further implications regarding data interpretation.

Even though it is generally understood that prolonged UV exposure may render biomaterials unsuitable for cell culture, there are few reports documenting in a quantitative fashion how this common sterilization procedure affects cell behavior such as morphology. Hence, we employed a full factorial design (Table 1b) to investigate the combined effects of substrate UV exposure, cell media composition, and the cell seeding density on the morphological features of MSCs seeded on both micro- and macroscale tctPS substrates. For the following studies, densities of 5000 and 10000 cells/cm^2 were instead used in order to avoid cellular confluence within tctPS microchannels, which facilitated single cell morphological analysis.

When seeded into tctPS microchannels, MSCs exhibited changes in morphological features that depended significantly on the substrate UV exposure duration, the initial cell seeding density, as well as the cell media composition (serum concentration). From a global analysis of the morphological data (Table 3), increasing the duration of substrate UV exposure decreased both the area and eccentricity but increased the form factor and solidity of attached MSCs. As expected, the addition of serum largely conferred effects (increased area and eccentricity but decreased circularity and solidity) that oppose those of substrate UV exposure on MSC morphology. Following similar trends, increasing the initial seeding density from 5000 to 10000 cells/cm^2 led to a general increase in cell area and eccentricity and a decrease in solidity without affecting the form factor. It is likely that greater cell densities, similar to the addition of serum, improve cell spreading via paracrine and trophic signaling [28]. The morphology of MSCs from the tctPS microchannels at 5000 and 10000 cells/cm^2 seeding densities is shown in Figure 5 and 6, respectively.

For each serum concentration tested, MSCs seeded at both low and high densities showed reduced area and eccentricity on 16h UV tctPS surfaces when compared to their corresponding 4h UV and 0h UV counterparts (Figure7A and B). A dose-dependent behavior for cellular eccentricity was demonstrated by MSCs cultured in 16% serum but not by those in 2% serum nor serum-free conditions, suggesting interaction effects between growth media conditions and substrate modifications. Indeed, while the form factor and solidity of MSCs seeded in 16h UV tctPS microchannels were usually greater than those observed for 4h UV and 0h UV groups cultured at the same serum concentrations, the effects of UV on morphology were largely attenuated by increasing amounts of serum (Figure 7C and 7D). These effects are likely explained by the provision of cytokines and adsorption of proteins via the serum-containing media that enhance cell spreading [29]. A main and cross effects analysis was also performed (Supplemental Table 4) to formally characterize such interactions between experimental factors. Briefly, MSCs seeded at a lower density (5000 cells/cm^2) and cultured at lower serum concentrations were confirmed to be more sensitive in their morphological response to changes in substrate properties in tctPS microchannels (Supplemental Figure 3).

While the presented data captured the population morphological response of MSCs to the various substrates (Table 1), the data also highlighted some heterogeneity of the employed MSC population given the relatively large standard deviations in the measured shape features. Cell heterogeneity is widely recognized as a significant obstacle toward the development of cell-based therapies [30]. As MSC morphology may reflect their phenotypic or functional capabilities upon differentiation [5], it is necessary to improve methods to characterize MSC morphological heterogeneity due to substrate modifications. To accomplish this, PCA was performed on the tctPS microscale dataset using 14 total morphological shape features (Supplemental Table 1), where the PC1 scores (47.9% total variance) were then plotted against the PC2 scores (29% total variance). From the PC scores plot (Figure 7E), the heterogeneity of the MSC morphological data is readily apparent. Despite their relatively heterogeneous distributions, data from the PCA largely confirms the morphological trends observed for the MSCs seeded within tctPS microchannels as affected by serum concentration and substrate UV treatment duration. They also emphasize that MSCs seeded at the lower density in tctPS microchannels were much more responsive to

changes in substrate properties. Of note, these results illustrate the successful adaptation of our simple microfluidic platform into a high-dimensional analytical framework for identifying morphological characteristics in response to specific substrate and culture conditions. Future research endeavors may utilize this platform to interrogate the morphological heterogeneity of stem cells in order to identify conditions that aid in the translation of emerging cell-based therapies into clinical success.

Evaluation of MSC morphological response to unexposed and UV-exposed tctPS macroscale culture and comparison with microscale culture using PCA

Understanding how MSCs interact with their substrates within more relevant microscale environments versus conventional macroscale platforms will be important for the design of controlled translational studies of higher clinical value. Given that the scale of the culture environment can significantly alter cellular responses to stimuli, a subset of the experimental groups tested in microchannels were also assessed in parallel utilizing standard open-well tissue culture plates (Table 1c). While keeping the serum concentration of the media fixed at 16%, it was shown that the morphology of MSCs cultured in macroscale were generally sensitive to differences in substrate UV exposure in a similar fashion to those in microchannels (Figure 8). Despite this similarity between micro- and macroscale conditions, modifying the initial cell seeding density for MSCs on well plates actually resulted in opposite effects when compared to the same experimental subset in microchannels (Supplemental Table 5). For the well plates, MSCs seeded at higher density (10000 versus 5000 cells/cm^2) maintained lower spreading areas and eccentricity, whereas in microchannels MSCs seeded at lower density showed greater spreading areas and eccentricity. The morphology of MSCs from the macroscale tctPS groups is shown in Figure 9. An analysis of the main and cross effects (Supplemental Table 5) additionally revealed that MSCs seeded at lower density in microchannels were more sensitive (in terms of spreading area) to substrate modifications (in this case UV treatment) whereas the opposite was true for MSCs seeded on conventional macroscopic well plates (Supplemental Figure 4). This observation has important corollaries for the translation of traditional macroscopic cell culture to more physiologically relevant microscale platforms, especially for diagnostic or phenotypic assay development purposes.

PCA was also performed on a larger and complex dataset (comprising 14 variables, which are fully described in Supplemental Table 1) in order to more comprehensively describe differences in overall MSC morphology between experimental groups. Morphological datasets from the tctPS microchannel and the tctPS macroscale well-plate experiments that were run in parallel were both subjected to PCA. Specifically, PC1 and PC2 from the combined morphological dataset accounted for 37.7% and 34.1% of the total variance, respectively. PC1 scores were plotted against PC2 scores to visualize differences in overall cell morphology as affected by the cell seeding density and substrate UV exposure depending on the culture environment scale (Figure 10). From the PC scores plot for the tctPS microchannel data, there is a clear partitioning of the composite MSC morphological characteristics along PC1 and PC2 (which account for the most variance in the data) as influenced by substrate UV exposure duration. MSCs seeded at lower density (5000 versus 10000 cells/cm^2) appeared to show greater separation in composite morphology scores for

the different substrate UV treatments, corroborating main effects data indicating a greater sensitivity of the cells to their substrates when seeded at a lower density. For the corresponding experimental groups in macroscale, we observed a slight but similar separation in MSC morphology along PC2 as affected by UV substrate modification for MSCs seeded at 10000 cells/cm^2. However, such separation of the PC scores was not observed for MSCs seeded at the lower density. Together, these results further highlight the influence of scale on MSC behavior and the utility of microfluidic platforms for quantitatively characterizing and screening cell-substrate interactions, especially at single-cell resolutions.

Conclusion

While current cell-based assays predominantly rely on macroscale open-well platforms, microfluidic tools are quickly enabling the analysis of cells at physiologically relevant scales which may facilitate more rapid translation to clinical success. Indeed, the development of quantitative methods of analysis for interrogating cell behavior in microfluidic cell culture devices further facilitates their integration as standard biological tools for in a high-throughput fashion. Here, we examined and qualified the utility of passive pumping microfluidic platforms comprising conventional PS substrates as simple devices for high dimensional cell morphological analysis as a means for characterizing cell-substrate interactions. Using UV as a modality for substrate modification, we demonstrated that MSCs seeded in microfluidic devices exhibited differing morphological trends and enumerated their morphological responses depending on the type of PS used as the cell culture substrate. For bgPS microchannels, MSCs interacted dynamically with their substrates based on the duration of substrate UV exposure where short durations of prior UV exposure actually increased some attributes of cell morphology on bgPS. Although MSCs seeded in tctPS microchannels were less spread with longer durations of substrate UV exposure, increasing cell seeding density and serum concentration both conferred a rescuing effect on MSC spreading. We observed largely comparable trends in MSC morphological response to changes in substrate conditions between microscale and macroscale platforms, demonstrating the former as a viable high-throughput cell culture device for cell-based assays. Despite similar cell-substrate interactions in terms of morphology, MSCs seeded in microscale were more sensitive to changes in substrate properties and exhibited different interactions with their substrates depending on cell seeding density, highlighting the importance of scale in developing cell-based therapies. Collectively, these data illustrate the ability to efficiently adapt microfluidic devices as simple platforms for performing high throughput, high dimensional analyses of MSC morphology as a quantitative method for studying cell-material interactions.

Supplementary Material

Refer to Web version on PubMed Central for supplementary material.

Acknowledgements

The authors would like to acknowledge Drs. Guo-Chiuan Hung, Heba Degheidy and Kimberly Benton for reviewing the manuscript. This work is supported in part by Dr. Johnny Lam’s appointment to the Research

Participation Program at CBER administered by the Oak Ridge Institute for Science and Education through the US Department of Education and US Food and Drug Administration. This work was also partially supported by the Food and Drug Administration Modernizing Science grant program, research funds from the Division of Cell and Gene Therapies, the University of Wisconsin Carbone Cancer Center Cancer Center Support Grant P30 CA014520, NIH T32 HL07899, and the University of Wisconsin Advanced Opportunity Fellowship through the Graduate Engineering Research Scholars (GERS) Program.

References

1. Tavassoli M; Crosby WH, Transplantation of marrow to extramedullary sites. Science 1968, 161 (3836), 54–6. [PubMed: 4871792]
2. (a)Caplan AI; Dennis JE, Mesenchymal stem cells as trophic mediators. J Cell Biochem 2006, 98 (5), 1076–84; [PubMed: 16619257] (b) Ranganath SH, et al., Harnessing the mesenchymal stem cell secretome for the treatment of cardiovascular disease. Cell Stem Cell 2012, 10 (3), 244–58. [PubMed: 22385653]
3. Bianco P, et al., The meaning, the sense and the significance: translating the science of mesenchymal stem cells into medicine. Nat Med 2013, 19 (1), 35–42. [PubMed: 23296015]
4. (a) Bellayr IH, et al., Gene markers of cellular aging in human multipotent stromal cells in culture. Stem Cell Res Ther 2014, 5 (2), 59; [PubMed: 24780490] (b) Lo Surdo JL, et al., Automated microscopy as a quantitative method to measure differences in adipogenic differentiation in preparations of human mesenchymal stromal cells. Cytotherapy 2013, 15 (12), 1527–40; [PubMed: 23992827] (c) Poon Z, et al., Bone marrow regeneration promoted by biophysically sorted osteoprogenitors from mesenchymal stromal cells. Stem Cells Transl Med 2015, 4 (1), 56–65. [PubMed: 25411477]
5. (a) Marklein RA, et al., High Content Imaging of Early Morphological Signatures Predicts Long Term Mineralization Capacity of Human Mesenchymal Stem Cells upon Osteogenic Induction. Stem Cells 2016, 34 (4), 935–47; [PubMed: 26865267] (b) Treiser MD, et al., Cytoskeleton-based forecasting of stem cell lineage fates. Proc Natl Acad Sci U S A 2010, 107 (2), 610–5. [PubMed: 20080726]
6. Cote AJ, et al., Single-cell differences in matrix gene expression do not predict matrix deposition. Nat Commun 2016, 7, 10865. [PubMed: 26936319]
7. Young EW; Beebe DJ, Fundamentals of microfluidic cell culture in controlled microenvironments. Chem Soc Rev 2010, 39 (3), 1036–48. [PubMed: 20179823]
8. (a) Duncombe TA, et al., Microfluidics: reframing biological enquiry. Nat Rev Mol Cell Biol 2015, 16 (9), 554–67; [PubMed: 26296163] (b) Whitesides GM, The origins and the future of microfluidics. Nature 2006, 442 (7101), 368–73. [PubMed: 16871203]
9. (a) Domenech M, et al., Cellular observations enabled by microculture: paracrine signaling and population demographics. Integr Biol (Camb) 2009, 1 (3), 267–74; [PubMed: 20011455] (b) Warrick J, et al., High-throughput microfluidics: improved sample treatment and washing over standard wells. Lab Chip 2007, 7 (3), 316–21; [PubMed: 17330162] (c) Yu H, et al., Diffusion dependent cell behavior in microenvironments. Lab Chip 2005, 5 (10), 1089–95. [PubMed: 16175265]
10. (a) Montanez-Sauri SI, et al., Automation of three-dimensional cell culture in arrayed microfluidic devices. J Lab Autom 2011, 16 (3), 171–85; [PubMed: 21609700] (b) Puccinelli JP, et al., Automated high-throughput microchannel assays for cell biology: Operational optimization and characterization. JALA Charlottesv Va 2010, 15 (1), 25–32. [PubMed: 20209121]
11. Paguirigan AL, et al., Expanding the available assays: adapting and validating In-Cell Westerns in microfluidic devices for cell-based assays. Assay Drug Dev Technol 2010, 8 (5), 591–601. [PubMed: 20658945]
12. Walker G; Beebe DJ, A passive pumping method for microfluidic devices. Lab Chip 2002, 2 (3), 131–4. [PubMed: 15100822]
13. Kim J, et al., Hydrophobic recovery of polydimethylsiloxane elastomer exposed to partial electrical discharge. Journal of Colloid and Interface Science 2000, 226 (2), 231–236.
14. (a) Paguirigan AL; Beebe DJ, Microfluidics meet cell biology: bridging the gap by validation and application of microscale techniques for cell biological assays. Bioessays 2008, 30 (9), 811–21;

[PubMed: 18693260] (b) Halldorsson S, et al., Advantages and challenges of microfluidic cell culture in polydimethylsiloxane devices. Biosens Bioelectron 2015, 63, 218–31. [PubMed: 25105943]

15. Public Health Service, C. f. D. C. a. P., National Institutes of Health, Primary containment for biohazards: Selection, installation and use of biological safety cabinets. 5th ed.; Services, U. S. D. o. H. a. H., Ed. 2009.
16. Carpenter AE, et al., CellProfiler: image analysis software for identifying and quantifying cell phenotypes. Genome Biol 2006, 7 (10), R100. [PubMed: 17076895]
17. Gelman A; Hill J, Data analysis using regression and multilevelhierarchical models. Cambridge University Press New York, NY, USA: 2007; Vol. 1.
18. Curtis AS, et al., Adhesion of cells to polystyrene surfaces. J Cell Biol 1983, 97 (5 Pt 1), 1500–6. [PubMed: 6355120]
19. Baker SC, et al., Characterisation of electrospun polystyrene scaffolds for three-dimensional in vitro biological studies. Biomaterials 2006, 27 (16), 3136–46. [PubMed: 16473404]
20. Fisher M; Solursh M, The influence of the substratum on mesenchyme spreading in vitro. Exp Cell Res 1979, 123 (1), 1–13. [PubMed: 488173]
21. Ranby BG; Rabek JF, Photodegradation, photo-oxidation, and photostabilization of polymers. New York, Wiley: 1975.
22. Nurmukhametov R, et al., Fluorescence and absorption of polystyrene exposed to UV laser radiation. Journal of Applied Spectroscopy 2006, 73 (1), 55–60.
23. (a) Morris EJ, The practical use of ultraviolet radiation for disinfection purposes. Med Lab Technol 1972, 29 (1), 41–7; [PubMed: 5038923] (b) Yen S, et al., Treating cell culture media with UV irradiation against adventitious agents: minimal impact on CHO performance. Biotechnol Prog 2014, 30 (5), 1190–5; [PubMed: 25044686] Wekhof A. Pulsed UV Disintegration (PUVD): a new sterilisation mechanism for packaging and broad medical-hospital applications; The First International Conference on Ultraviolet Technologies; Washington D.C., USA. June 14–16; 2001. Washington D.C., USA, 2001.
24. Folch A, et al., Microfabricated elastomeric stencils for micropatterning cell cultures. J Biomed Mater Res 2000, 52 (2), 346–53. [PubMed: 10951374]
25. Yu H, et al., Understanding microchannel culture: parameters involved in soluble factor signaling. Lab Chip 2007, 7 (6), 726–30. [PubMed: 17538714]
26. Ramsey WS, et al., Surface treatments and cell attachment. In Vitro 1984, 20 (10), 802–8. [PubMed: 6519665]
27. (a) Bretagnol F, et al., The effect of sterilization processes on the bioadhesive properties and surface chemistry of a plasma-polymerized polyethylene glycol film: XPS characterization and L929 cell proliferation tests. Acta Biomater 2008, 4 (6), 1745–51; [PubMed: 18676191] (b) Noah EM, et al., Impact of sterilization on the porous design and cell behavior in collagen sponges prepared for tissue engineering. Biomaterials 2002, 23 (14), 2855–61. [PubMed: 12069325]
28. McBeath R, et al., Cell shape, cytoskeletal tension, and RhoA regulate stem cell lineage commitment. Dev Cell 2004, 6 (4), 483–95. [PubMed: 15068789]
29. (a) Grinnell F; Feld MK, Fibronectin adsorption on hydrophilic and hydrophobic surfaces detected by antibody binding and analyzed during cell adhesion in serum-containing medium. J Biol Chem 1982, 257 (9), 4888–93; [PubMed: 7068668] (b) Arima Y; Iwata H, Effect of wettability and surface functional groups on protein adsorption and cell adhesion using well-defined mixed self-assembled monolayers. Biomaterials 2007, 28 (20), 3074–82; [PubMed: 17428532] (c) Wei J, et al., Influence of surface wettability on competitive protein adsorption and initial attachment of osteoblasts. Biomed Mater 2009, 4 (4), 045002; [PubMed: 19525576] (d) Dewez JL, et al., Competitive adsorption of proteins: key of the relationship between substratum surface properties and adhesion of epithelial cells. Biomaterials 1999, 20 (6), 547–59. [PubMed: 10213358]
30. (a) Ho AD, et al., Heterogeneity of mesenchymal stromal cell preparations. Cytotherapy 2008, 10 (4), 320–30; [PubMed: 18574765] (b) Pevsner-Fischer M, et al., The origins of mesenchymal stromal cell heterogeneity. Stem Cell Rev 2011, 7 (3), 560–8.

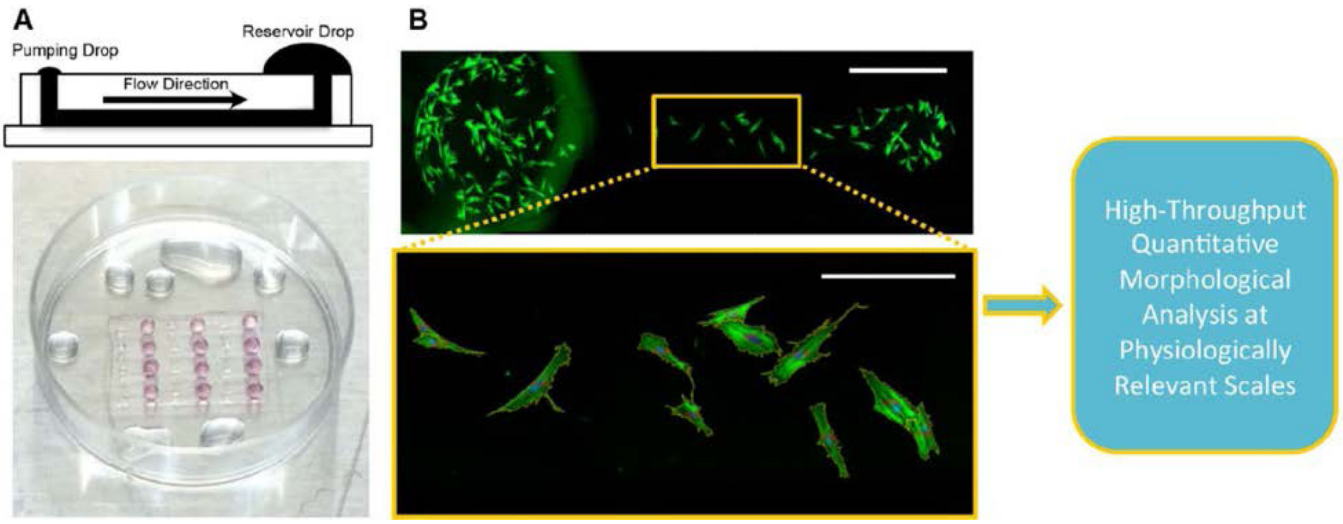

Figure 1:

A schematic of the quantitative high-dimensional morphological analysis of MSCs using simple passive-pumping microfluidic platforms is shown. (A) MSCs were seeded into microfluidic devices comprising straight channel arrays bonded to various PS substrates driven by passive pumping, (B) fixed and stained for automated imaging (actin – green; nuclei – blue) after 24h and then subjected to high dimensional morphological analysis. The scale bars for the top and bottom (magnified) images are 1,000 and 250 microns, respectively.

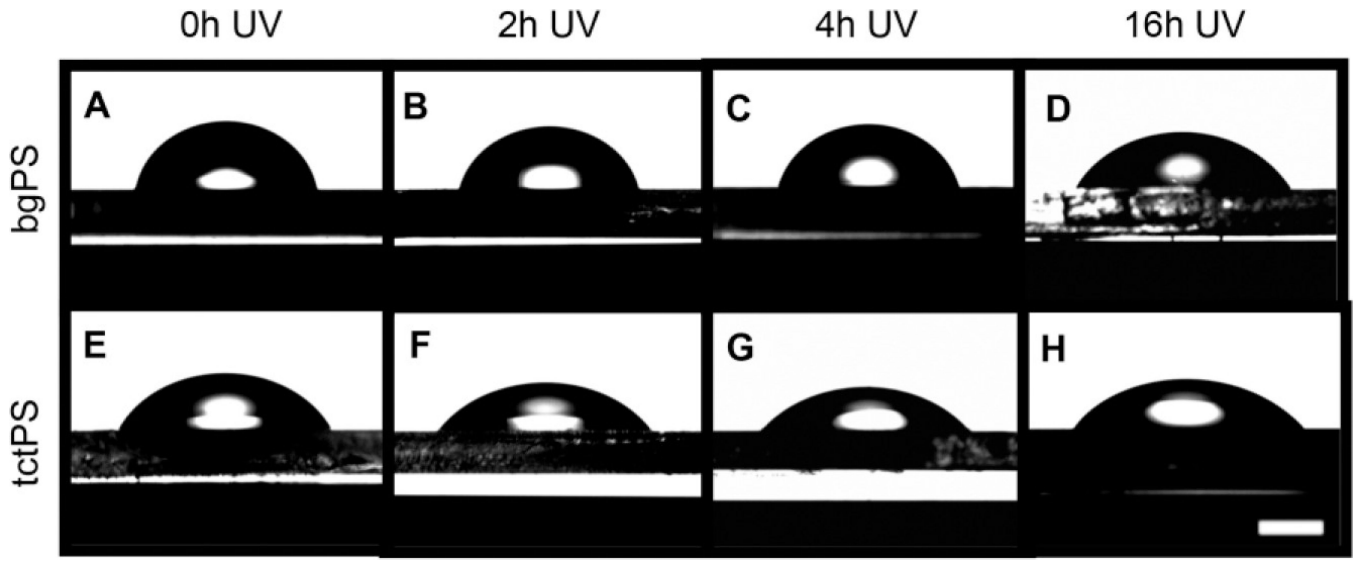

Figure 2:

Water droplets were formed on (A-D) untreated bacterial grade (bgPS; n=4) and (E-H) tissue culture-treated PS (tctPS; n=4) substrates irradiated with UV for (A, E) 0h, (B, F) 2h, (C, G) 4h, and (D, H) 16h. Contact angles were obtained using a goniometer. Scale bar is 1.5 mm.

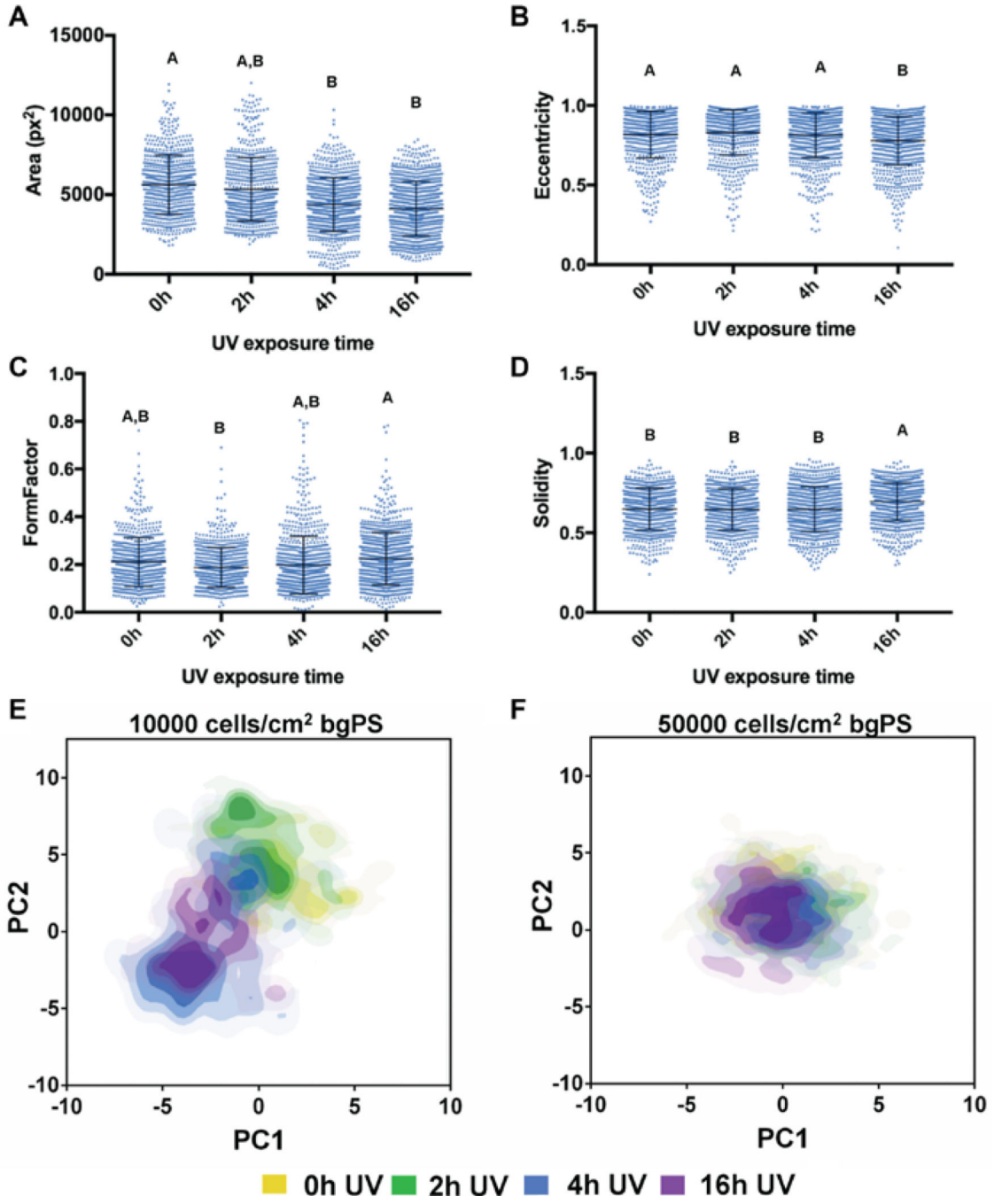

Figure 3:

Dot plots of the measured cell shape features representing single-cell morphological (A) area (pixel), (B) eccentricity, (C) form factor, and (D) solidity are shown for MSCs seeded at both low and high densities on bgPS 0hUV (n=679), bgPS 2hUV (n=685), bgPS 4hUV (n=823) and bgPS 16hUV (n=899) microchannels. For each morphological feature, groups not connected by the same letters (A, B, C, and D) are significantly different ($p<0.05$). Scores plots generated from the PCA of the bgPS microchannel morphological datasets are shown for both (E) 10000 and (F) 50000 cells/cm^2. Each plotted point represents the

composite morphological score of a single cell, where the yellow, green, blue, and violet colored dots represent tctPS substrates that were exposed to 0h, 2h, 4h, and 16h of UV prior to cell seeding, respectively.

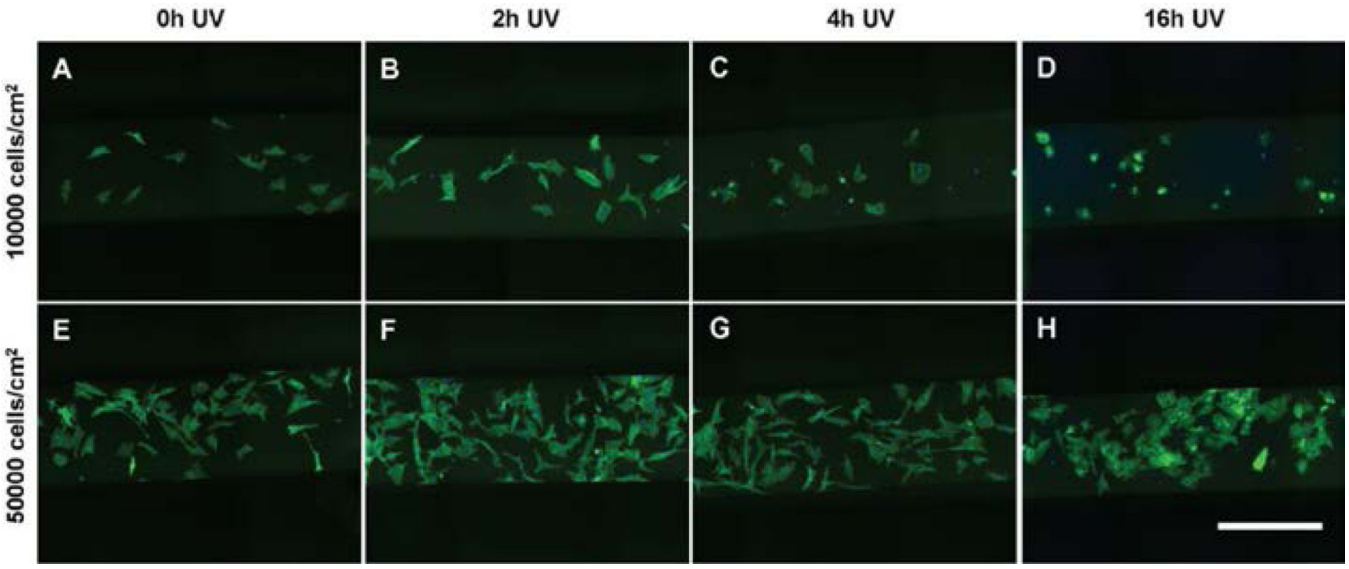

Figure 4:

The morphology of MSCs seeded at (A-D) 10000 and (E-H) 50000 cells/cm^2 within bgPS microchannels is shown for bgPS substrates that were previously subjected to (A, E) 0h, (B, F) 2h, (C, G) 4h, and (D, H) 16h of UV exposure prior to cell seeding. MSCs were stained for actin (green) and nuclei (blue). Scale bar is 500 microns.

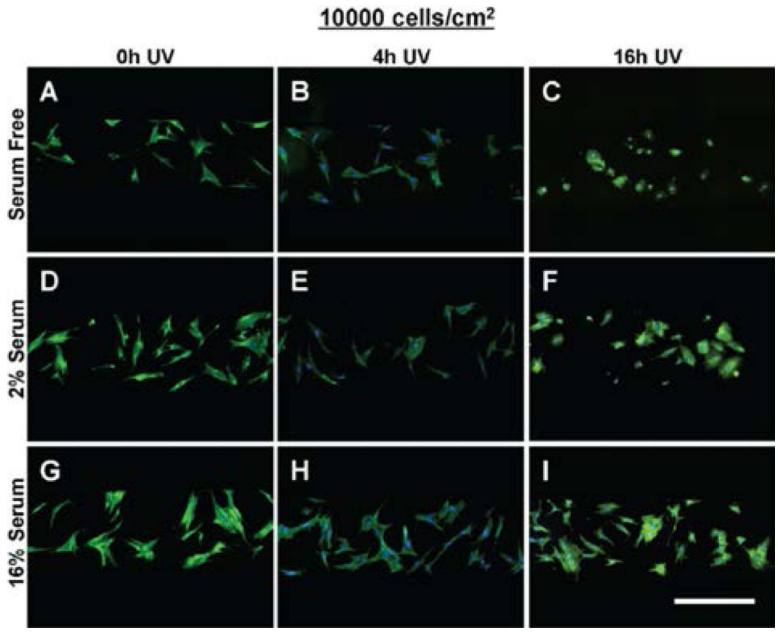

Figure 5:

The morphology of MSCs seeded at 5000 cells/cm^2 within tctPS microchannels grown in (A-C) serum free, (D-F) 2% serum, and (G-I) 16% serum conditions is shown for tctPS substrates that were previously subjected to (A, D, G) 0h, (B, E, H) 4h, and (C, ,G, I) 16h of UV exposure prior to cell seeding. MSCs were stained for actin (green) and nuclei (blue). Scale bar is 500 microns.

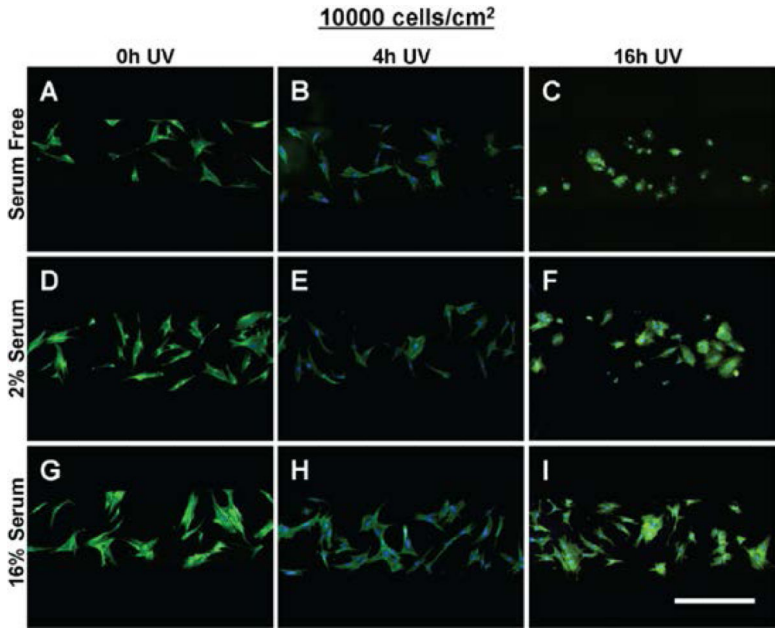

Figure 6:

The morphology of MSCs seeded at 10000 cells/cm^2 within tctPS microchannels grown in (A-C) serum free, (D-F) 2% serum, and (G-I) 16% serum conditions is shown for tctPS substrates that were previously subjected to (A, D, G) 0h, (B, E, H) 4h, and (C, ,G, I) 16h of UV exposure prior to cell seeding. MSCs were stained for actin (green) and nuclei (blue). Scale bar is 500 microns.

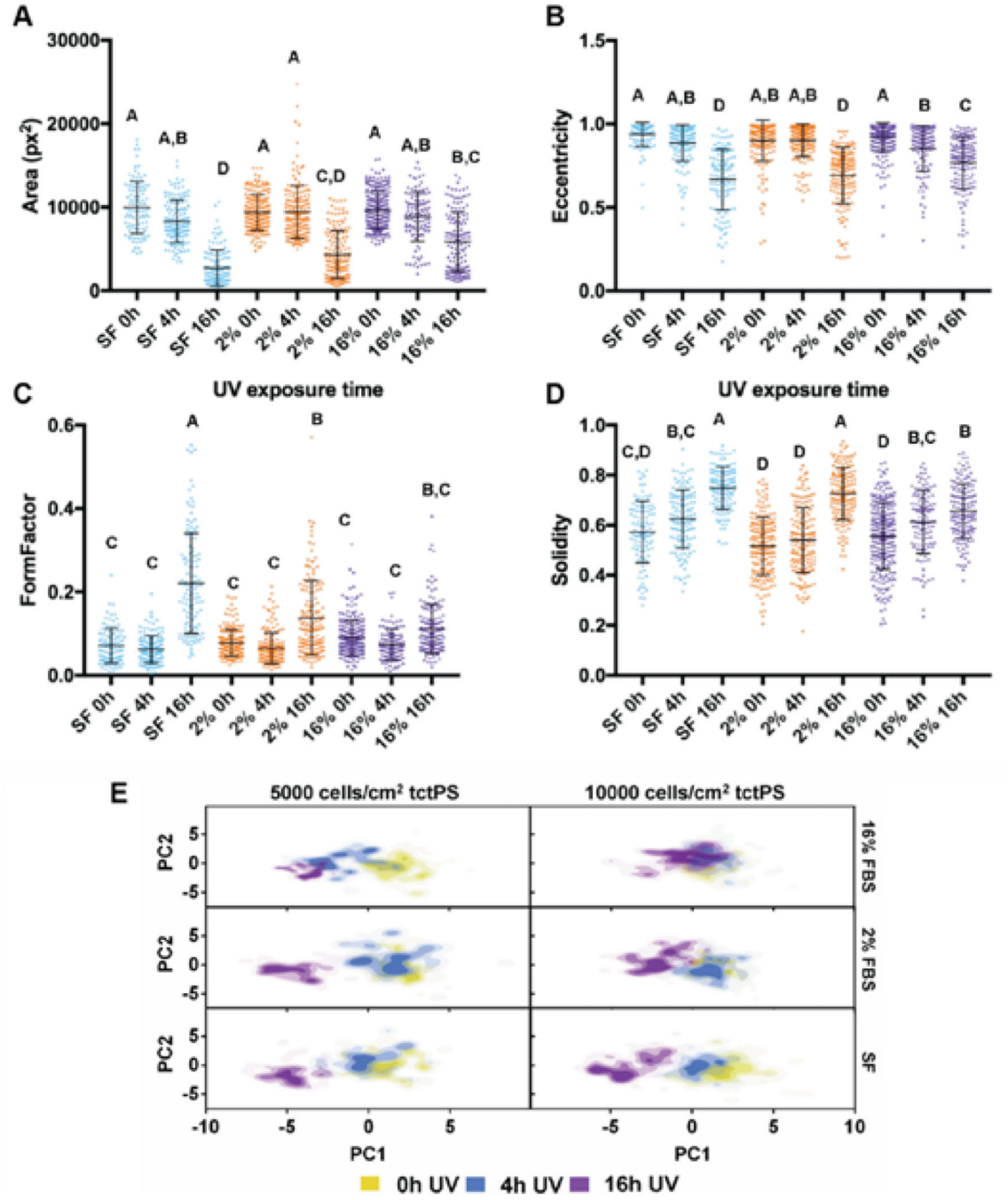

Figure 7:

Dot plots of the indicated cell shape features representing single-cell morphological (A) area (pixel), (B) eccentricity, (C) form factor, and (D) solidity are shown for MSCs seeded on tctPS microchannels. Morphological data are shown for MSCs seeded at both low and high densities for each UV exposure time at each serum concentration. The groups are as follows: SF 0hUV (n=102), SF 4hUV (n=135), SF 16hUV (n=122), 2% 0hUV (n=182), 2% 4hUV (n=166), 2% 16hUV (n=154), 16% 0hUV (n=256), 16% 4hUV (n=112), and 16% 16hUV (n=144). For each morphological feature, groups not connected by the same letters (A, B, C,

and D) are significantly different ($p<0.05$). (E) Scores plots generated from the PCA of the tctPS microchannel morphological datasets are shown for both 5000 and 10000 cells/cm^2 and at the indicated serum concentrations. Each plotted point represents the composite morphological score of a single cell, where the yellow, blue, and violet colored dots represent tctPS substrates that were exposed to 0h, 4h, and 16h of UV prior to cell seeding, respectively.

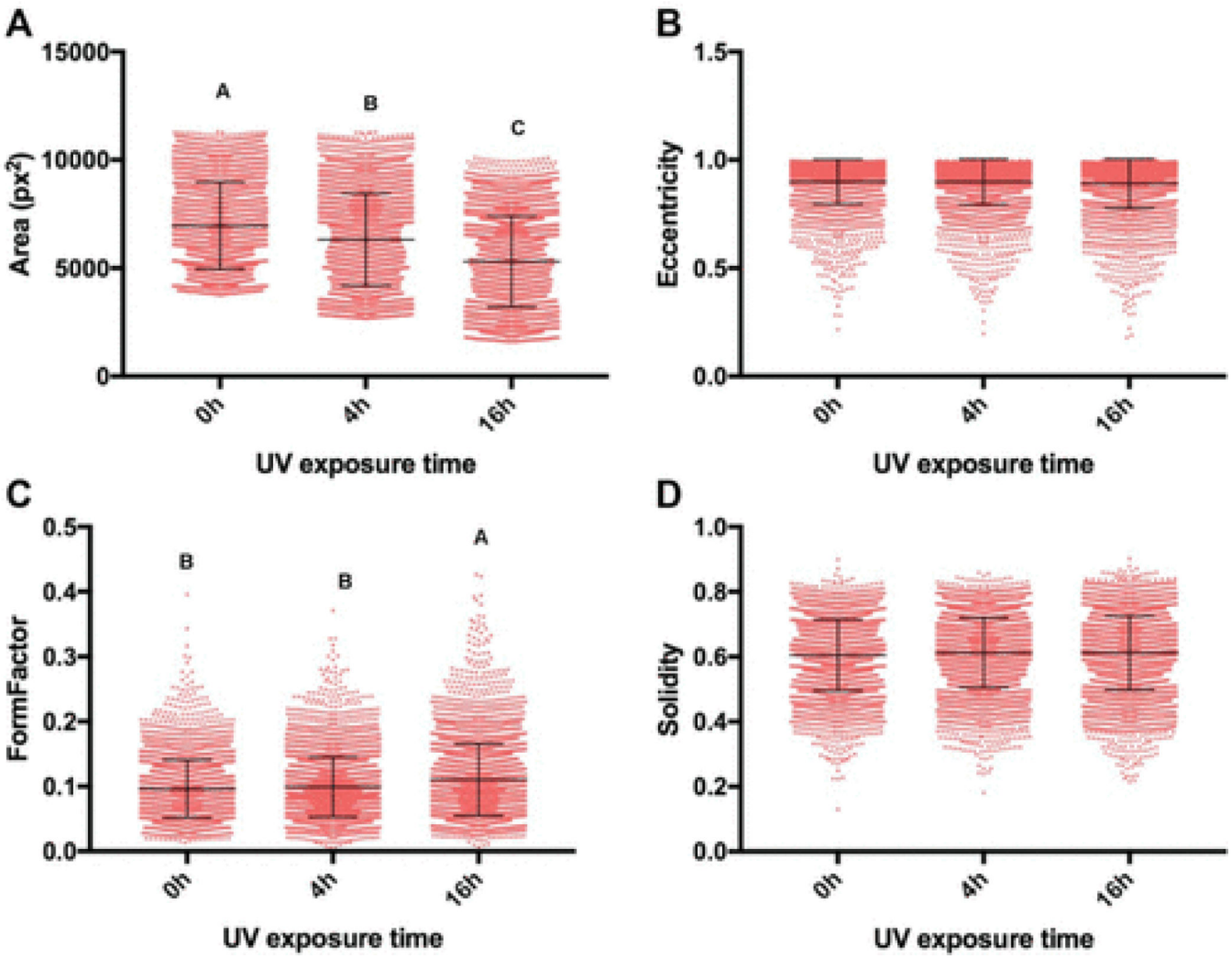

Figure 8:

Dot plots of the measured cell shape features representing single-cell morphological (A) area (pixel), (B) eccentricity, (C) form factor, and (D) solidity are shown for MSCs seeded at both low and high densities on standard tctPS 0hUV (n=2864), tctPS 4hUV (n=3721), and tctPS 16hUV (n=3679) well plates. For each morphological feature, groups not connected by the same letters (a, b, c, and d) are significantly different ($p<0.05$).

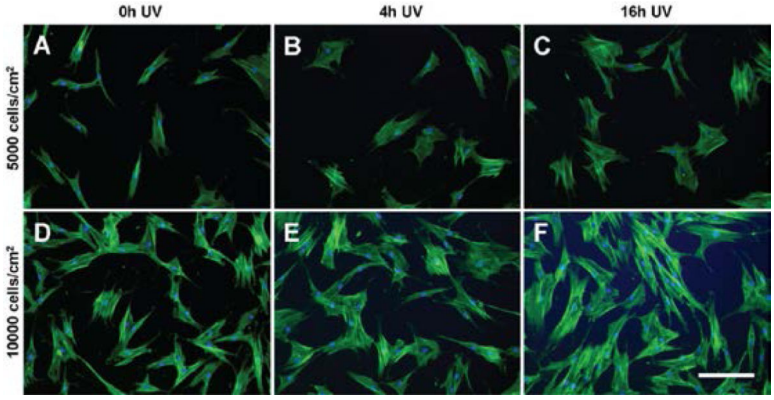

Figure 9:

The morphology of MSCs seeded at (A-C) 5000 and (D-F) 10000 cells/cm^2 on standard tctPS well plates is shown for tctPS substrates that were previously subjected to (A, D) 0h, (B, E) 4h, and (C, F) 16h of UV exposure prior to cell seeding. MSCs were stained for actin (green) and nuclei (blue). Scale bar is 200 microns.

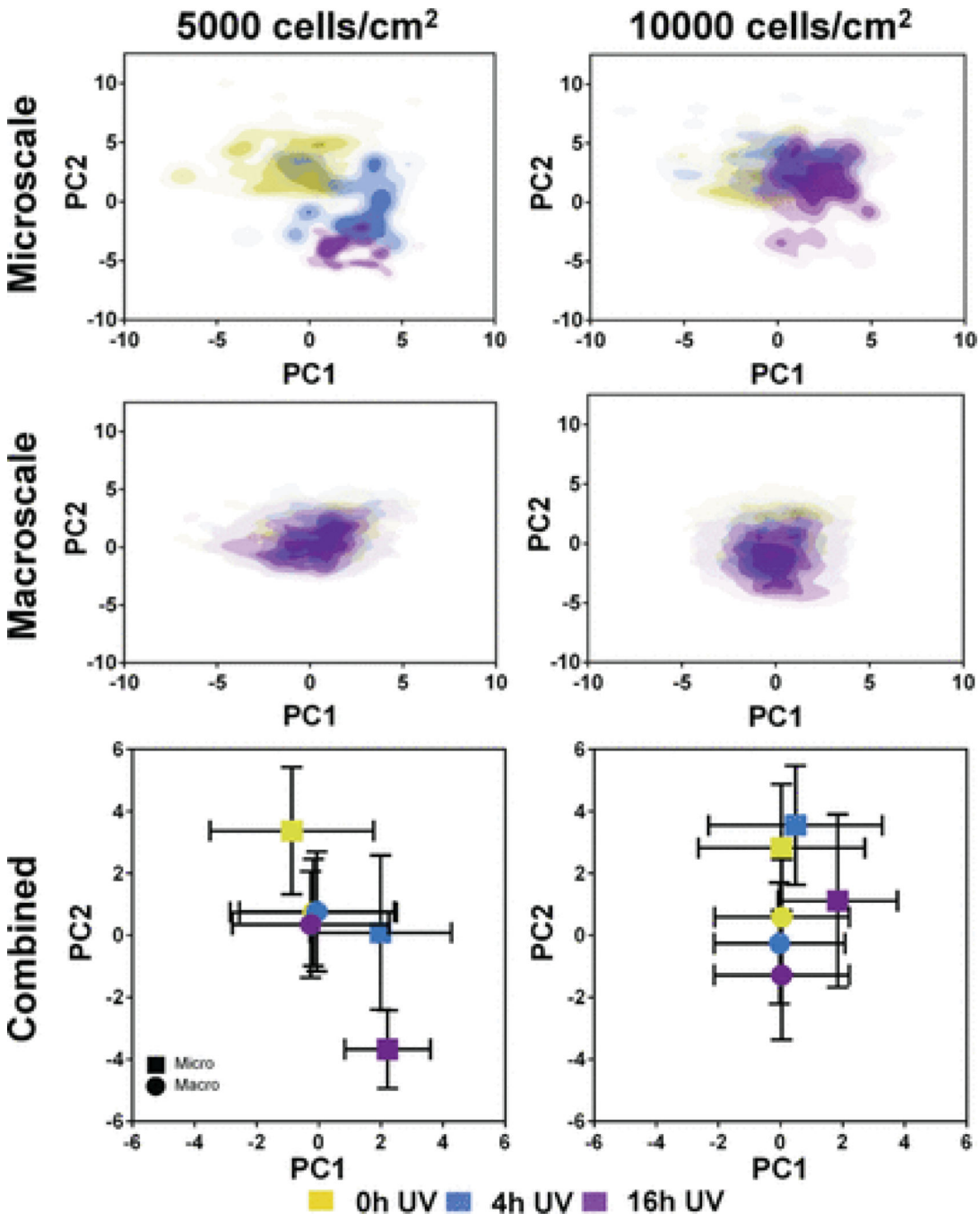

Figure 10:

Scores plots generated from the PCA of the tctPS microchannel and macroscale tctPS well plate MSC morphological datasets are shown. For the separate microscale and macroscale plots at both 5000 and 10000 cells/cm^2, each plotted point represents the composite morphological score of a single cell, where the yellow, blue, and violet colored dots represent tctPS substrates that were exposed to 0h, 4h, and 16h of UV prior to cell seeding, respectively. For the combined plots, each plotted point (■ for microscale; ● for

macroscale) represents the averaged PC1 and PC2 scores for each UV treatment group and their respective standard deviations.

Table 1:

Full factorial design to investigate effects of cell seeding density, growth media composition, and UV surface treatment on the adhesion and morphology of MSCs. n represents the number of cells evaluated per UV treatment group for each study.

a.) Group	Cell Density		UV Treatment
bgPS 0hUV	10000 or 50000 cells/cm^2		0h (*n=679*)
bgPS 2hUV	10000 or 50000 cells/cm^2		2h (*n=685*)
bgPS 4hUV	10000 or 50000 cells/cm^2		4h (*n=823*)
bgPS 16hUV	10000 or 50000 cells/cm^2		16h (*n=899*)
b.) Group	**Cell Density**	**Serum Content**	**UV Treatment**
SF 0hUV	5000 or 10000 cells/cm^2	SF	0h (*n=102*)
SF 4hUV	5000 or 10000 cells/cm^2	SF	4h (*n=135*)
SF 16hUV	5000 or 10000 cells/cm^2	SF	16h (*n=122*)
2% 0hUV	5000 or 10000 cells/cm^2	2% FBS	0h (*n=182*)
2% 4hUV	5000 or 10000 cells/cm^2	2% FBS	4h (*n=166*)
2% 16hUV	5000 or 10000 cells/cm^2	2% FBS	16h (*n=154*)
16% 0hUV	5000 or 10000 cells/cm^2	16% FBS	0h (*n=256*)
16% 4hUV	5000 or 10000 cells/cm^2	16% FBS	4h (*n=112*)
16% 16hUV	5000 or 10000 cells/cm^2	16% FBS	16h (*n=144*)
c.) Group	**Cell Density**		**UV Treatment**
16% 0hUV wp	5000 or 10000 cells/cm^2		0h (*n=2864*)
16% 4hUV wp	5000 or 10000 cells/cm^2		4h (*n=3721*)
16% 16hUV wp	5000 or 10000 cells/cm^2		16h (*n=3679*)

Table 2:

Measured water contact angles and droplet heights on the various PS substrates as a function of UV exposure duration. For each substrate type, groups not connected by the same letter (*a*, *b*, or *c*) are significantly different ($p<0.05$). For each UV exposure duration, * indicates a significant difference between the types of PS substrate.

Substrate (n=4)	UV Treatment	Contact Angle (°)	Droplet Height (mm)
bgPS	0h	$80.84\pm2.02^{a,*}$	$1.83\pm0.05^{a*}$
bgPS	2h	$77.65\pm2.45^{a,b,*}$	$1.74\pm0.04^{a,b*}$
bgPS	4h	$73.23\pm1.14^{b*}$	$1.68\pm0.01^{b*}$
bgPS	16h	$57.28\pm2.88^{c*}$	$1.41\pm0.06^{c*}$
tctPS	0h	58.50 ± 2.12^{a}	1.42 ± 0.06^{a}
tctPS	2h	48.38 ± 1.23^{b}	1.25 ± 0.02^{b}
tctPS	4h	50.03 ± 2.27^{b}	1.24 ± 0.05^{b}
tctPS	16h	48.80 ± 2.13^{b}	1.23 ± 0.03^{b}

Table 3:

Global analysis of the morphological data from all MSCs seeded in tctPS microchannels. For each cell morphological feature, the data are presented as mean ± the standard error. Within each factor, morphological features not connected by the same letter (*a*, *b*, or *c*) are significantly different ($p<0.05$).

Factor (Cell Seeding Density)	**Area**	**Eccentricity**	**Form Factor**	**Solidity**
5000 cells/cm^2 (n=459)	7127.3±103.3^a	0.818±0.008^a	0.104±0.004	0.620±0.007^a
10000 cells/cm^2 (n=914)	8142.9±206.6^b	0.857±0.005^b	0.097±0.002	0.602±0.004^b
Factor (Serum Concentration)	**Area**	**Eccentricity**	**Form Factor**	**Solidity**
Serum free (n=359)	6881.8±211.8^b	0.827±0.009^b	0.119±0.006^a	0.652±0.007^a
2% serum (n=502)	7847.0±161.1^{a,b}	0.837±0.007^{a,b}	0.092±0.003^b	0.588±0.007^b
16% serum (n=512)	8406.8±143.8^a	0.863±0.006^a	0.093±0.002^b	0.597±0.006^b
Factor (UV Exposure Duration)	**Area**	**Eccentricity**	**Form Factor**	**Solidity**
0h UV (n=540)	9606.0±103.9^a	0.918±0.004^a	0.082±0.002^b	0.546±0.005^c
4h UV (n=413)	8916.3±145.5^a	0.883±0.006^b	0.067±0.002^b	0.587±0.006^b
16h UV (n=420)	4391.3±156.2^b	0.711±0.008^c	0.153±0.005^a	0.708±0.005^a